

High Magnetic Field Effects on Biradical Lifetimes: Evaluation of Magnetic Field Dependence and Chain Length Dependence Using Calculated *g* and Hyperfine Tensors

Yutaka Mouri, Yoshihisa Fujiwara,* Takeshi Aoki, Hiroshi Yoshida, Kazunari Naka, Yuriko Aoki,[1] Hiroaki Yonemura,[2] Sunao Yamada,[2] Takeharu Haino, Yoshimasa Fukazawa, and Yoshifumi Tanimoto

Graduate School of Science, Hiroshima University, Kagamiyama, Higashi-hiroshima 739-8526

[1]Interdisciplinary Graduate School of Engineering Sciences, Kyushu University, Kasuga-kouen, Kasuga 816-8580

[2]Faculty of Engineering, Kyushu University, Hakozaki, Higashi-ku, Fukuoka 812-8581

Received December 1, 2004; E-mail: fuji0710@sci.hiroshima-u.ac.jp

The *g* and hyperfine tensors of radicals were theoretically estimated by quantum chemical calculations, and compared with experimentally obtained ones. From the comparison, it was found that the theoretically calculated tensors can reproduce the experimental ones with accuracy. By using those tensors, therefore, high magnetic field dependences of the lifetimes of biradicals, which were generated by a photo-induced electron transfer in α-cyclodextrin inclusion complexes of chain-linked molecules of phenothiazine–$(CH_2)_n$–viologen (PhnV^{2+}, $n = 12$, 10, and 8) and carbazole–$(CH_2)_{12}$–viologen (Cz12V^{2+}), were quantitatively analyzed on the basis of the relaxation mechanism of the generated bi-cationic biradicals (Ph$^{\bullet+}n$V$^{\bullet+}$ and Cz$^{\bullet+}$12V$^{\bullet+}$). The analysis conclusively showed that two extremely small correlation times of each radical motion were still necessary for reversals characteristic of the high magnetic field dependences, and also that the order of the obtained correlation time was Cz$^{\bullet+}$ > V$^{\bullet+}$ > Ph$^{\bullet+}$. The order in the correlation time was discussed while referring to the rigidity of the radical frameworks.

During the last decade, many investigations of magnetic field effects (MFEs) on the lifetimes (decays) of biradicals and radical pairs have been vigorously carried out in a high magnetic field region beyond 10 T in order to discover new MFEs specified in a high magnetic field.[1–5] As a result, it has been found that a reversal very frequently appears in the magnetic field dependences (MFDs) of the lifetimes (decays), and that the MFDs are interpreted in terms of the relaxation mechanism.[1–6] From quantitative studies according to the relaxation mechanism, it has been demonstrated that the simultaneous operation of three interactions modulating the spin–lattice relaxation (SLR) processes is responsible for the reversal, namely, the anisotropic Zeeman (δg) and anisotropic hyperfine (δhf) interactions on individual component radicals, and the electron dipole–dipole (dd) interaction between the component radicals of a biradical and/or a radical pair. With increasing the magnetic field, the δg interaction operates to decrease the lifetime in a higher magnetic field region, usually above 3 T, whereas the δhf and dd interactions operate to increase it in a relatively lower region of 0.1–2 T. Therefore, the δg interaction has been found to be indispensable for the reversal, since only this interaction among them decreases the lifetime. On the other hand, the three interactions are closely relevant to the radical motions modulating SLR to affect the radical lifetimes. The origins of the motions are normally discussed based on the correlation times of the motions. The correlation times have often been estimated analytically by simulating the obtained MFDs according to the relaxation mechanism. However, the estimated correction times have been extremely small compared with those calculated by applying the radical whole size to the conventionally used Stokes–Einstein–Debye (SED) equation.[7,8] This discrepancy is received at present by interpreting that the small correlation times are attributable to local motions existing in the radical frameworks. However, it may not be denied that some unknown parameters, including the correlation time, cause an ambiguity in the values during the analysis. Hence, to improve the accuracy in the parameters, we have attempted to evaluate the *g* and *hf* tensors necessary for estimating the δg and δhf interactions with a calculation program constructed based on theory of quantum chemistry, and thereby to decrease the number of unknown parameters during the analysis. In the present work, we have checked the reproducibility of those tensors by the calculation program, and then applied them to simulations of the MFDs to obtain the correlation times. The reaction used here was an electron-transfer reaction in α-cyclodextrin inclusion complexes of chain-linked molecules of phenothiazine (Ph) or carbazole (Cz) as an electron donor and viologen (V^{2+}) as an acceptor. Our group already reported on an extremely small correlation time (1 ps) in the Ph12V^{2+} system, and tentatively assigned it to the local motion, such as a butterfly motion existing in a Ph ring.[9] Here, we confirm the extremely small correlation time, even when using the theoretically calculated tensors, and consider the origin by comparing two molecules having different electron donors of Ph and Cz, of which the rigidity seems to be higher than Ph.

Published on the web May 6, 2005; DOI 10.1246/bcsj.78.804

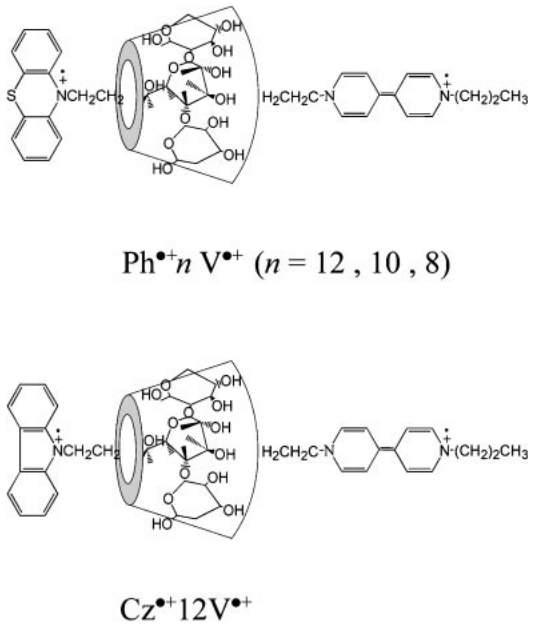

Fig. 1. Biradical structures of $Ph^{\bullet+}nV^{\bullet+}$ (n = 12, 10, and 8) and $Cz^{\bullet+}12V^{\bullet+}$.

1. Experimental

Materials. Chain-linked compounds, ($Phn V^{2+}2Br^{-}$ (n = 12, 10, 8) and $Cz12V^{2+}2Br^{-}$), were synthesized according to standard procedures.[10] α-Cyclodextrin (Nacalai Tesque, GR grade) was used as received. Xanthone (XO) (Nacalai Tesque, GR grade) was utilized as a triplet sensitizer after several recrystallizations. Distilled and deionized water was used as the solvent. The concentration of the chain-linked compounds were ca. 0.2 mM. We used 10 mM and 2 mM α-cyclodextrin aqueous solutions in experiments concerning the triplet sensitization of $Ph12V^{2+}$ and $Cz12V^{2+}$ with XO and the direct laser excitation of $Phn V^{2+}$, respectively. The sample solutions were deaerated by several freeze–pump–thaw cycles prior to laser experiments.

Apparatus. The transient absorption ascribed to the component radical ($V^{\bullet+}$) in $Ph^{\bullet+}nV^{\bullet+}$ and $Cz^{\bullet+}12V^{\bullet+}$ (Fig. 1) was monitored at 390 nm in high magnetic fields by a pulse-magnet laser flash photolysis system, described elsewhere.[11] The exciting light source was a Nd:YAG laser (Spectra Physics, GCR-11-1) (355 nm, 10 ns fwhm). All measurements were performed at room temperature.

Calculations. Quantum chemical calculations of the g and hyperfine (hf) tensors were carried out with a calculation program (Gaussian03W)[12] for radicals, illustrated in Fig. 2.[13] Both structural optimization of the radicals and a subsequent tensor calculation were performed by the B3LYP method of density functional theory. The basis set 6-31+G(d) was used for the calculation. The reproducibility was checked by comparing them with ones so far reported.[13] For a model calculation simulating the observed MFDs of the above-mentioned chain-linked compounds, the tensors of the *N*-methylphenothiazine radical cation (Me–$Ph^{\bullet+}$), the *N*,*N*′-dimethylviologen radical cation (Me_2–$V^{\bullet+}$), and the *N*-methylcarbazole radical cation (Me–$Cz^{\bullet+}$) were calculated with Gaussian03W, while taking the structures of generated biradicals ($Ph^{\bullet+}nV^{\bullet+}$ and $Cz^{\bullet+}12V^{\bullet+}$) into account.

The inter-radical distance (R) related to the dd interaction was calculated by the mixed Monte Carlo/stochastic dynamics method as well as in a previous study.[9]

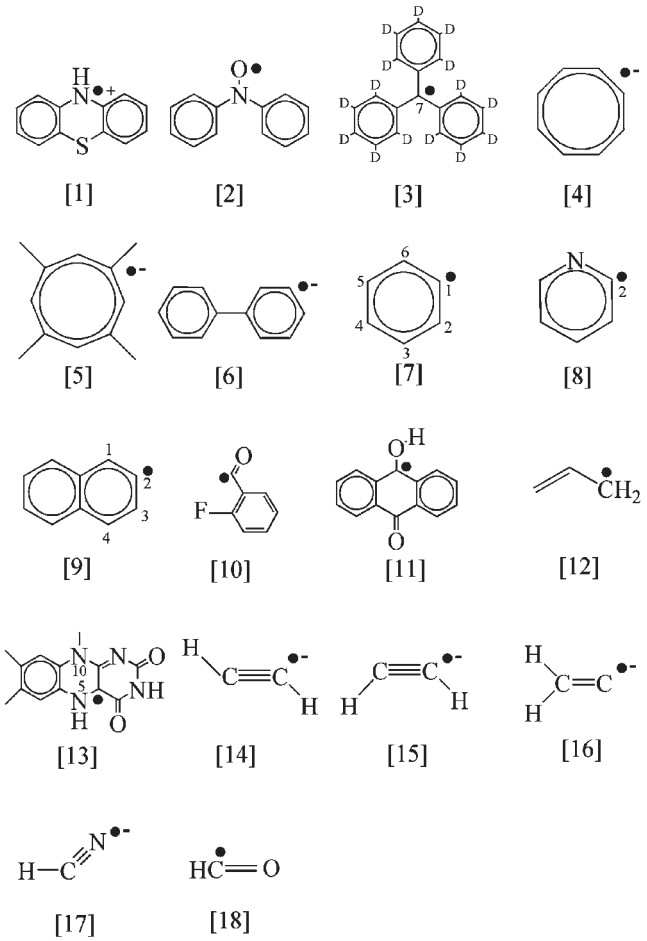

Fig. 2. Radical structures utilized in quantum chemical calculations for checking the reproducibility of the g and hf tensors.

2. Results and Discussion

2.1 High Magnetic Field Effects on Biradical Lifetimes and the Mechanisms. As already reported,[9,14] the electron transfer between a donor of Ph (or Cz) and an acceptor of V^{2+} in $Phn V^{2+}$ and $Cz12V^{2+}$ takes place in water upon 355 nm laser excitation, resulting in the generation of triplet biradicals (BRs) composed of radical cations of $Ph^{\bullet+}$ (or $Cz^{\bullet+}$) and $V^{\bullet+}$. However, it was found that the generation quantum yield (Φ_{BR}) of the initially-populated triplet biradical was as small as ca. 0.1 in $Cz^{\bullet+}12V^{\bullet+}$, in contrast to ca. 0.7 in $Ph^{\bullet+}12V^{\bullet+}$, judging from the fluorescence lifetimes (τ_F*) of the excited singlet states (^{1}Ph* and ^{1}Cz*) in the parent molecules ($Ph12V^{2+}$ and $Cz12V^{2+}$) and the rate constants (k_{ISC}*) of the intersystem crossing (ISC) to the corresponding excited triplet states (^{3}Ph* and ^{3}Cz*).[10,15] In fact, the transient absorption signal intensity of $Cz^{\bullet+}12V^{\bullet+}$ was too weak to obtain the biradical lifetime precisely. In this study, therefore, the triplet sensitization of $Cz12V^{2+}$ with XO as a triplet sensitizer was carried out to generate the initially populated triplet biradical efficiently.[16] The molecule of XO was suitable as a triplet sensitizer owing both to the exited triplet energy (E_T = 309 kJ/mol) being higher than that (E_T = 294 kJ/mol) of Cz and to the sole excitation of XO at 355 nm of the laser wavelength. $Ph12V^{2+}$ was also sensitized with XO for a comparison.

The reaction scheme in the triplet sensitization in case of $Ph12V^{2+}$ is shown as follows:

$$XO \xrightarrow{h\nu 355\ nm} {}^1XO^* \xrightarrow{ISC} {}^3XO^*, \quad (1)$$

$${}^3XO^* + Ph12V^{2+} \xrightarrow{\text{Triplet Sensitization}} XO + {}^3Ph^*12V^{2+}, \quad (2)$$

$${}^3Ph^*12V^{2+} \xrightarrow{\text{Electron Transfer}} {}^3[Ph^{\bullet+}12V^{\bullet+}], \quad (3)$$

$${}^3[Ph^{\bullet+}12V^{\bullet+}] \xrightarrow{ISC} {}^1[Ph^{\bullet+}12V^{\bullet+}], \quad (4)$$

$${}^1[Ph^{\bullet+}12V^{\bullet+}] \longrightarrow Ph12V^{2+}, \quad (5)$$

$${}^3[Ph^{\bullet+}12V^{\bullet+}] \xrightarrow{Ph12V^{2+}} Ph^{\bullet+}12V^{2+} \text{ and } Ph12V^{\bullet+}, \quad (6)$$

$${}^3[Ph^{\bullet+}12V^{\bullet+}] \xrightarrow{\text{SOC-induced recombination}} Ph12V^{2+}. \quad (7)$$

Upon 355 nm laser excitation, the excited triplet state ($^3XO^*$) of XO is generated (Eq. 1). The excited triplet state ($^3Ph^*12V^{2+}$) of $Ph12V^{2+}$, sensitized by $^3XO^*$, gives rise to electron transfer reaction from $^3Ph^*$ to V^{2+} to yield the triplet bi-cationic biradical ($^3[Ph^{\bullet+}12V^{\bullet+}]$) (Eqs. 2 and 3). It undergoes ISC to the singlet one ($^1[Ph^{\bullet+}12V^{\bullet+}]$) (Eq. 4), and finally returns to the ground state of $Ph12V^{2+}$ by reverse electron transfer (Eq. 5). The triplet biradical partly reacts to form the corresponding mono-radical cations of $Ph^{\bullet+}12V^{2+}$ and $Ph12V^{\bullet+}$ (Eq. 6), and partly disappears via spin–orbit-coupling (SOC)-induced recombination to the ground state (Eq. 7). Since an external magnetic field affects both ISC to $^1[Ph^{\bullet+}12V^{\bullet+}]$ and the SLR processes to the triplet sub-states of $^3[Ph^{\bullet+}12V^{\bullet+}]$, the biradical lifetime changes drastically with increasing the magnetic field.

The transient absorption time profiles were monitored at 390 nm, where the characteristic absorption band assigned to $V^{\bullet+}$ appeared. On the other hand, the time needed for the triplet energy transfer was obtained to be 1.22 μs in $Ph^{\bullet+}12V^{\bullet+}$ and 1.96 μs in $Cz^{\bullet+}12V^{\bullet+}$, respectively, from the decay profiles at 600 nm assigned to $^3XO^*$. Hence, in order to evaluate the biradical lifetime, the time profiles at 390 nm were analyzed with a two-exponential function for a consecutive reaction including the rate constant ($1.22^{-1} \times 10^6\ s^{-1}$ in $Ph^{\bullet+}12V^{\bullet+}$ and $1.96^{-1} \times 10^6\ s^{-1}$ in $Cz^{\bullet+}12V^{\bullet+}$) of the energy transfer process. This is the reason why the biradical lifetime at 0 T was not obtained. Figure 3 shows MFDs of the biradical lifetimes of $Ph^{\bullet+}12V^{\bullet+}$ (Fig. 3a) and $Cz^{\bullet+}12V^{\bullet+}$ (Fig. 3b) in magnetic fields of up to 14 T, except that at 0 T. In these biradicals, reversals consisting of an increase and the succeeding decrease in the lifetime were observed. The reversals took place at around 1 T in $Ph^{\bullet+}12V^{\bullet+}$ and 4 T in $Cz^{\bullet+}12V^{\bullet+}$, respectively. Further, the extent of the reversals of $Ph^{\bullet+}12V^{\bullet+}$ was much larger than that of $Cz^{\bullet+}12V^{\bullet+}$. This fact indicates that a moiety of $Ph^{\bullet+}$ is responsible for the large extent of the reversal.

In these MFDs, the MFE on the lifetime below ca. 0.1 T is explained by the isotropic *hf* interaction of biradicals. As already discussed in the literature,[1–6,9] on the other hand, all of the reversals observed above ca. 0.1 T are interpreted by the relaxation mechanism in the biradical SLR, namely, the δg and δhf interactions on the component radicals and the dd interaction on the biradical. Only the former accelerates the SLR to decrease the lifetime, while the two latter ones decelerate the relaxation to increase the lifetime. Further, from the theory of the relaxation mechanism and experiments so far carried out

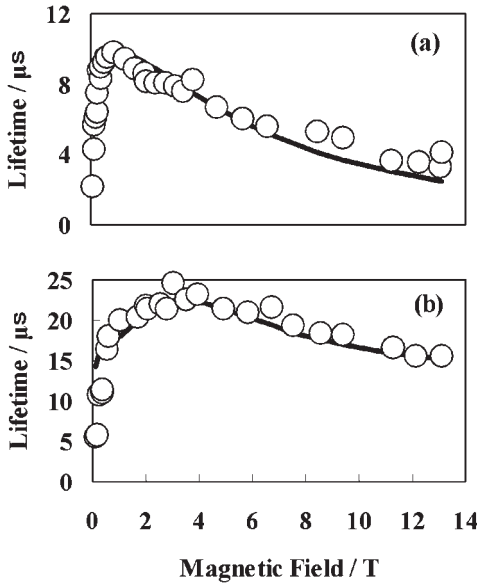

Fig. 3. Observed (○) and finally simulated (▬) MFDs of the biradical lifetimes in (a) $Ph^{\bullet+}12V^{\bullet+}$ and (b) $Cz^{\bullet+}12V^{\bullet+}$. The observed MFDs were obtained by the triplet sensitization with XO. The parameters for the δg and δhf interactions in the simulated curves are $(g{:}g) = 181.8 \times 10^{-7}$, $(H_{loc}{:}H_{loc}) = 1.52\ mT^2$, and $\tau_c = 0.115$ ps for $Ph^{\bullet+}$, $(g{:}g) = 20.01 \times 10^{-7}$, $(H_{loc}{:}H_{loc}) = 2.31\ mT^2$, and $\tau_c = 0.75$ ps for $V^{\bullet+}$, and $(g{:}g) = 1.478 \times 10^{-7}$, $(H_{loc}{:}H_{loc}) = 2.26\ mT^2$, and $\tau_c = 2.4$ ps for $Cz^{\bullet+}$, respectively. The parameters for the dd interaction commonly used in the simulated curves are $\overline{R^6} = 11.0 \times 10^6\ Å^6$ and $\tau_{c12} = 374$ ps. The k_T value is 8.5×10^4 and $1.00 \times 10^4\ s^{-1}$ for $Ph^{\bullet+}12V^{\bullet+}$ and $Cz^{\bullet+}12V^{\bullet+}$, respectively.

in many biradicals and radical pairs, it is experimentally found that the former effectively operates in magnetic fields higher than ca. 3 T, while the two latter ones do so in magnetic fields of ca. 0.1–2 T. Therefore, the decreases in the lifetimes observed above 1 T of $Ph^{\bullet+}12V^{\bullet+}$ and above 4 T of $Cz^{\bullet+}12V^{\bullet+}$ are due to the δg interaction, while the increases in ca. 0.1–1 T of $Ph^{\bullet+}12V^{\bullet+}$ and in ca. 0.1–3 T of $Cz^{\bullet+}12V^{\bullet+}$ are due to the combination of the δhf and dd interactions. In a previous paper describing $Ph^{\bullet+}12V^{\bullet+}$,[9] a quantitative analysis of MFD was carried out based on a theory of the relaxation mechanism in order to elucidate the validity of the assignment stated above, and also to assign the origin of the radical motion causing the reversal. In the result, an unusually small rotational correlation time (1 ps) of the radical motion probably attributable to the local motions, such as a butterfly motion of a Ph ring, was indicated to be important for the appearance of the reversal. However, the *g* and *hf* tensors of $V^{\bullet+}$, which were essential for the quantitative analysis, were unknown, and therefore were also estimated through the simulation process of the MFD as well as the unknown correlation time. Therefore, some extent of ambiguity still remained in the *g* tensor, the *hf* tensor, and the correlation times obtained. In the present work, in order to retain a theoretical meaning toward the unknown tensors, they were estimated by using a program recently improved for calculating the *g* tensor.

Table 1. Observed and Calculated Principal Values of the *g* and *hf* Tensors

Radical No.[a)]	*g* Tensor			*hf* Tensor	
	g_{XX} g_{YY} g_{ZZ}			A_{XX}/mT A_{YY}/mT A_{ZZ}/mT	
	Observed[b)]	Calculated	Nuclear type[c)]	Observed[b)]	Calculated
1	2.0072	2.00770	N	1.70	1.42
	2.0060	2.00639		0.13	0.10
	2.0024	2.00189		0.13	0.093
2	2.0092	2.00990	N	2.38	2.10
	2.0056	2.00529		0.36	0.14
	2.0022	2.00212		0.19	0.11
3	2.0028	2.00274	^{13}C(7)	6.00	6.26
	2.0026	2.00274		0.86	1.3
	2.0020	2.00217		0.68	1.3
4	2.00341	2.00344	H	0.359	0.545
	2.00341	2.00273		0.313	0.422
	2.00271	2.00273		0.313	0.0837
5	2.00298	2.00280			
	2.00298	2.00275			
	2.00247	2.00275			
6	2.00334	2.00340			
	2.00262	2.00255			
	2.00230	2.00182			
7	2.0034	2.00303	H(2,6)	2.19	2.20
	2.0023	2.00214		1.54	1.56
	2.0014	2.00153		1.49	1.52
			H(3,5)	0.66	0.77
				0.61	0.50
				0.50	0.47
			H(4)	0.25	0.25
				0.20	0.21
				0.12	0.15
			^{13}C(1)	17.4	17.5
				10.7	11.2
				10.7	10.6
8	2.0020	2.00339	N	3.55	3.58
	2.0010	2.00211		2.73	3.08
	2.0010	2.00037		2.73	2.95
			^{13}C(2)	20.0	21.4
				15.5	16.1
				15.5	15.7
9	2.0030	2.00301	H(1)	2.01	2.43
	2.0023	2.00199		1.39	1.79
	2.0014	2.00173		1.32	1.75
			H(3)	2.41	2.01
				1.79	1.37
				1.72	1.33
			H(4)	0.690	0.741
				0.620	0.461
				0.470	0.436
10	2.0040	2.00454	^{13}C(α)	17.86	16.37
	2.0024	2.00115		13.71	11.98
	1.9961	1.99647		13.32	11.90
11	2.0067	2.00502			
	2.0044	2.00441			
	2.0021	2.00216			

Continued on next page.

Continued.

12	2.0031	2.00292			
	2.0026	2.00282			
	2.0023	2.00221			
13	2.00431	2.00451	N(5)	1.53	1.48
	2.00360	2.00403		−0.06	0.06
	2.00217	2.00202		−0.06	0.05
			N(10)	0.83	0.73
				0.04	0.07
				0.04	0.05
			H(5)	−0.30	−0.07
				−0.89	−1.05
				−1.33	−1.39
14	2.0027	2.00271	H	5.3	5.32
	2.0023	2.00178		4.7	4.52
	2.0011	2.00080		4.3	4.17
15	2.0032	2.00266	H	6.8	6.85
	2.0023	2.00231		6.6	6.21
	2.0008	2.00068		6.1	5.96
			^{13}C	15.0	14.1
				12.2	11.8
				11.9	11.7
16	2.0031	2.00314	H	5.9	5.46
	2.0023	2.00219		5.7	5.03
	2.0008	2.00112		5.5	4.99
17	2.0051	2.00330	H	14.17	11.3
	2.0021	2.00203		13.53	11.0
	1.9994	1.99842		13.44	10.9
			^{13}C	8.87	9.20
				6.92	7.45
				6.53	7.31
			N	2.11	2.27
				−0.02	0.10
				−0.06	0.08
18	2.0037	2.00450	H	13.5	13.6
	2.0023	2.00161		12.3	12.5
	1.9948	1.99539		12.0	12.2
			^{13}C	15.6	16.7
				12.2	12.4
				11.4	12.3

a) The numbers and structures are illustrated in Fig. 2. b) The observed data were taken from Ref. 13. c) For example, H(2,6) means the nuclear type (H) concerned with the *hf* interaction and the location number (2 and 6) in the radical. In the case of no location number, the location is on the atom attached a closed circle showing an electron in Fig. 2.

2.2 Reproducibility of the *g* and Hyperfine Tensors by Quantum Chemical Calculations. Table 1 gives principal values in the *g* and *hf* tensors calculated by quantum chemical calculations, compared with the experimentally observed ones of eighteen radicals. Figure 4 illustrates plots of the calculated principal values versus the observed ones. Since one radical has three principal values toward the *x*, *y*, and *z* directions specified as the molecular axes, the figures are composed of fifty-four plots. Taking the structures of $Ph^{\bullet+}nV^{\bullet+}$ and $Cz^{\bullet+}12V^{\bullet+}$ into account, the radicals having a π-molecular orbit spread into radical sites were utilized in the calculation. Additionally, the radicals consisting of light atoms of H, D, C, N, and O were used. Figure 4a displays the correlation in the *g* tensor. The straight line shows a fitted line (a scale factor of $f = 1.00$ and a coefficient of determination of $r^2 = 0.931$ in a fitting function of $y = fx$) obtained by the least-squares method. It was found that good reproducibility was obtained by the calculation method performed here. Also, in Fig. 4b for the *hf* tensors, good reproducibility is obtained. The scale factor and the coefficient of determination of the fitted straight line are $f = 1.02$ and $r^2 = 0.986$ in the fitting function of $y = fx$, respectively. For example, the closed circles (●) in Fig. 4 indicate plots of the phenothiazine radical cation with an N–H bond lying closely on a straight line. The calculated *g* and *hf* principal values ($g_{XX} = 2.00770$, $g_{YY} = 2.00639$, $g_{ZZ} = 2.00189$, $A^N_{XX} = 0.093$ mT, $A^N_{YY} = 0.10$ mT, $A^N_{ZZ} = 1.42$ mT) are very close to the observed ones ($g_{XX} = 2.0072$, $g_{YY} = 2.0060$, $g_{ZZ} = 2.0024$, $A^N_{XX} = 0.13$ mT, $A^N_{YY} = 0.13$ mT, $A^N_{ZZ} = 1.70$ mT), respectively.[13d] These results strongly suggest that the calculation method used here is capable for providing adequate tensors needed to simulate the MFDs of the biradical lifetimes with high accuracy. Therefore,

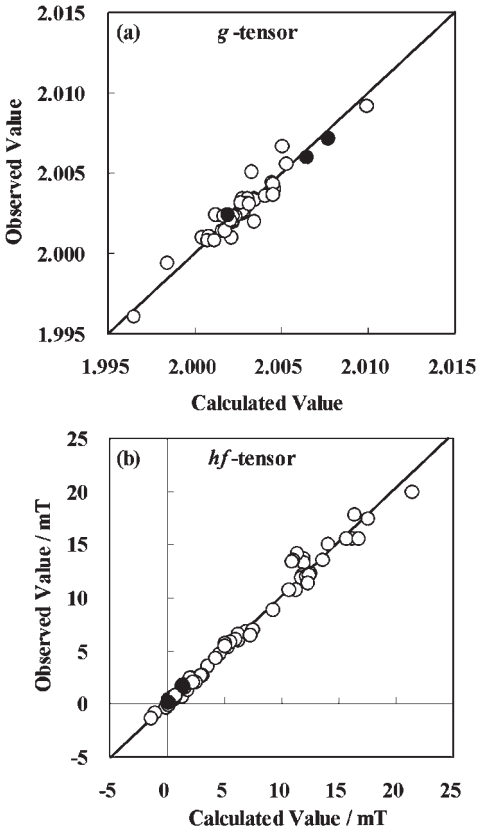

Fig. 4. Plots of the observed principal values versus the calculated ones in the (a) *g* and (b) *hf* tensors. The closed circles (●) in each figure indicate plots in the case of the phenothiazine radical cation with an N–H bond.

Table 2. Calculated *g* and *hf* Principal Values (g_{XX}, g_{YY}, g_{ZZ} and A^N_{XX}, A^N_{YY}, A^N_{ZZ}) and Inner Products ((*g*:*g*) and (H_{loc}:H_{loc})) of Me–Ph$^{\bullet+}$, Me_2–V$^{\bullet+}$, and Me–Cz$^{\bullet+}$

	Radical cation		
	Me–Ph$^{\bullet+}$	Me_2–V$^{\bullet+}$	Me–Cz$^{\bullet+}$
g_{XX}	2.00773	2.00390	2.00337
g_{YY}	2.00611	2.00293	2.00300
g_{ZZ}	2.00189	2.00190	2.00284
(*g*:*g*)	181.8×10^{-7}	20.01×10^{-7}	1.478×10^{-7}
A^N_{XX}/mT	0.165	0.160	0.205
A^N_{YY}/mT	0.175	0.177	0.209
A^N_{ZZ}/mT	1.68	2.03	2.05
(H_{loc}:H_{loc})/mT^2	1.52	2.31	2.26

The *hf* principal values are listed only for nitrogen atoms. All the principal values in the *g* and *hf* tensors are scaled with the scale factors of $f = 1.00$ and $f = 1.02$, respectively.

the *g* and *hf* principal values (g_{XX}, g_{YY}, g_{ZZ} and A^N_{XX}, A^N_{YY}, A^N_{ZZ}) of Me–Ph$^{\bullet+}$, Me_2–V$^{\bullet+}$, and Me–Cz$^{\bullet+}$ necessary for simulating the observed MFDs of Ph$^{\bullet+}$12V$^{\bullet+}$ and Cz$^{\bullet+}$12V$^{\bullet+}$ were calculated, as summarized in Table 2, together with the therewith inner products ((*g*:*g*) and (H_{loc}:H_{loc})). The values in Table 2 are scaled with the respective scale factors (*f*) for the *g* and *hf* tensors. As for the *hf* tensors, the principal values on nitrogen atoms listed in Table 2 were used to simulate the MFD due to the large contribution to the inner product. Table 2 predicts that the contributions of the respective interactions are on the orders of Me–Ph$^{\bullet+}$ > Me_2–V$^{\bullet+}$ > Me–Cz$^{\bullet+}$ in δg and Me_2–V$^{\bullet+}$ = Me–Cz$^{\bullet+}$ > Me–Ph$^{\bullet+}$ in δhf from the viewpoint of the magnitude in (*g*:*g*) and (H_{loc}:H_{loc}), respectively. However, it is not too much to say that the difference in (H_{loc}:H_{loc}) is negligibly small compared with (*g*:*g*).

2.3 Model Calculations and Interpretation of Magnetic Field Dependences Using the Calculated Tensors. According to the relaxation mechanism generally utilized above 0.1 T, as denoted in a previous study,[9] the decay rate constant (k_{BR}) of Ph$^{\bullet+}$12V$^{\bullet+}$, that is, the reciprocal of the biradical lifetime (τ_{BR}) is explicitly expressed as:

$$k_{BR} = \frac{1}{\tau_{BR}} = \sum_{i=1}^{2}\left[\left\{\frac{1}{2}(g{:}g)_i\beta^2B_0^2 + \frac{10}{9}g_i^2\beta^2(H_{loc}{:}H_{loc})_i\right\}\frac{\tau_{ci}}{5\hbar^2(1+\gamma_i^2B_0^2\tau_{ci}^2)}\right] + \frac{3\hbar^2\gamma_{12}^4}{2\overline{R^6}}\frac{\tau_{c12}}{5(1+\gamma_{12}^2B_0^2\tau_{c12}^2)} + k_T, \quad (8)$$

where the first term on the right-hand side of the equation consists of two anisotropic interactions of δg and δhf in each radical i, and the parameters of $(g{:}g)_i$ and $(H_{loc}{:}H_{loc})_i$ in it are inner products obtained from the δg and δhf tensors in the molecular-axis system of each radical i, respectively. The parameters of B_0, β, and $\hbar$ are the external magnetic field, the Bohr magneton, and Planck's constant divided by 2π, respectively. Other values of g_i, γ_i, and τ_{ci} for the radical i are the *g*-value, the magnetogyric ratio of the electron, and the correlation time of a radical Brownian motion modulating SLR, respectively. The second term means the dd interaction. The parameters in it were treated according to a previous work.[9] The correlation time (τ_{c12}) is calculated with the SED equation ($\tau_{c12} = 4\pi\eta a^3/(3kT)$).[7,8] Here, η is the viscosity of water at the absolute temperature (*T*), and *k* is the Boltzmann constant. The radius (*a*) is evaluated using the mean inter-radical distance ($\bar{R}$), which is obtained from the iteratively calculated *R* by the mixed Monte Carlo/stochastic dynamics method. The parameter $\overline{R^6}$ is the average of the sixth power of the calculated distance (*R*), and $\gamma_{12} = (\gamma_1\gamma_2)^{0.5}$. These values are summarized in Table 3 in addition to those for other biradicals of $n = 10$ and 8. The last term, k_T, is a total rate constant due to magnetic-field-independent deactivation processes (Eqs. 6 and 7) in biradicals. This term contributes to the lifetime in the same way regardless of the absence or presence of any magnetic fields. Since the ISC rate constant in Eq. 4 at 0 T, determined by the isotropic *hf* mechanism, is very large (typically ca. 10^8

Table 3. Parameters Necessary for Estimating the dd Interaction in Ph$^{\bullet+}$*n*V$^{\bullet+}$

Chain length *n*	$\overline{R^6}/10^6$ Å^6	$\bar{R}$/Å	τ_{c12}/ps
12	11.0[a)]	14.6[a)]	374[a)]
10	7.94	14.0	327
8	3.36	12.1	211

a) Taken from Ref. 9.

s^{-1}),[1–5] the lifetime (140 ns)[9] at 0 T of $Ph^{\bullet+}12V^{\bullet+}$ is explained by a combination of the processes (Eqs. 5–7), that is, the rate constant of the back electron transfer bringing with a chain motion (Eq. 5) and k_T (Eqs. 6 and 7). Roughly speaking, the lifetime at 0 T corresponds to a decay time of Eq. 5 because k_T is estimated to be as small as 10^4–10^6 s^{-1}.[9,17] On the other hand, in magnetic fields above ca. 0.1 T where Eq. 8 is available, the rate constant in Eq. 4 reduces to compare with k_T. Therefore, the lifetime is determined by a combination of the rate in Eq. 4 and k_T (Eqs. 6 and 7).

In the beginning a simulation for the MFD of $Ph^{\bullet+}12V^{\bullet+}$ in a previous study,[9] the parameters $\overline{R^6}$ and τ_{c12} for the dd interaction were firstly estimated as described above. Secondly, in estimating the δhf interaction of $Ph^{\bullet+}$, the values of $(g{:}g) = 125 \times 10^{-7}$ and $(H_{loc}{:}H_{loc}) = 1.65$ mT^2 were tentatively used from the experimental data ($g_{XX} = 2.0072$, $g_{YY} = 2.0060$, $g_{ZZ} = 2.0024$, $A^N{}_{XX} = 0.13$ mT, $A^N{}_{YY} = 0.13$ mT, $A^N{}_{ZZ} = 1.70$ mT) already reported for the phenothiazine radical cation,[13d] although this radical cation is exactly different in a structure from that of $Ph^{\bullet+}$, abbreviated here because it has an N–H bond, not an N–C one, in $Ph^{\bullet+}12V^{\bullet+}$. Therefore, the unknown parameters to be estimated were (i) τ_c for $Ph^{\bullet+}$, (ii) $(g{:}g)$, $(H_{loc}{:}H_{loc})$, and τ_c for $V^{\bullet+}$, and (iii) k_T for $Ph^{\bullet+}12V^{\bullet+}$, i.e., five parameters in the preceding study. Regardless of the five, however, the observed MFD was successfully simulated and the importance of an extremely small τ_c was pointed out.

In this study, the dd interaction was evaluated by the same method used in the previous study, as just mentioned above, and the necessary parameters were taken from Table 3. Additionally, the magnetic field region where the lifetime increases was found to be restricted to a narrow one lower than ca. 1 T in the case of $Ph^{\bullet+}12V^{\bullet+}$, indicating the dd interaction in fact operates only within the same narrow region. This fact means that the method of using the data calculated by the molecular dynamics is unlikely to cause any significant misconstruction in the interpretation of the MFD in > ca. 1 T, predominantly due to the δg interaction. On the other hand, the calculated $(g{:}g)$ and $(H_{loc}{:}H_{loc})$ in Table 2 were applied to both $Ph^{\bullet+}$ and $V^{\bullet+}$ in this study. In the result, the number of unknown parameters in Eq. 8 diminished from the five in the previous study to the three of (i) τ_c for $Ph^{\bullet+}$ and $V^{\bullet+}$ and (ii) k_T for $Ph^{\bullet+}12V^{\bullet+}$ in this study. Only those three parameters were varied during the fitting calculation to reproduce the observed MFD, as shown in Fig. 5. Similarly, in the case of $Cz^{\bullet+}12V^{\bullet+}$, the number of unknown parameters decreased from the seven, including $(g{:}g)$ and $(H_{loc}{:}H_{loc})$ for $Cz^{\bullet+}$ to the three of (i) τ_c for $Cz^{\bullet+}$ and $V^{\bullet+}$ and (ii) k_T for $Cz^{\bullet+}12V^{\bullet+}$. These decrements in the number are considered to definitely raise the reliability in the residual unknown parameters of τ_c and k_T.

Figure 5 displays several fitting curves (—) based on Eq. 8 to the observed MFD (○) in $Ph^{\bullet+}12V^{\bullet+}$ (Figs. 5a and 5b) and $Cz^{\bullet+}12V^{\bullet+}$ (Figs. 5c and 5d). In starting the model calculation for $Ph^{\bullet+}12V^{\bullet+}$, the necessary values of $(g{:}g)$ and $(H_{loc}{:}H_{loc})$ for the respective radicals were taken from Table 2. As for the k_T of $Ph^{\bullet+}12V^{\bullet+}$, commonly used in Figs. 5a and 5b, the value was finally set at 8.50×10^4 s^{-1} during the calculation to ascertain the contribution of τ_c of $Ph^{\bullet+}$ and $V^{\bullet+}$. The correlation time (τ_c) of $Ph^{\bullet+}$ was varied between 0.115 and 100 ps while fixing τ_c at 0.75 ps for $V^{\bullet+}$ in Fig. 5a. In Fig. 5b, τ_c of $V^{\bullet+}$ was varied between 0.1 and 100 ps while

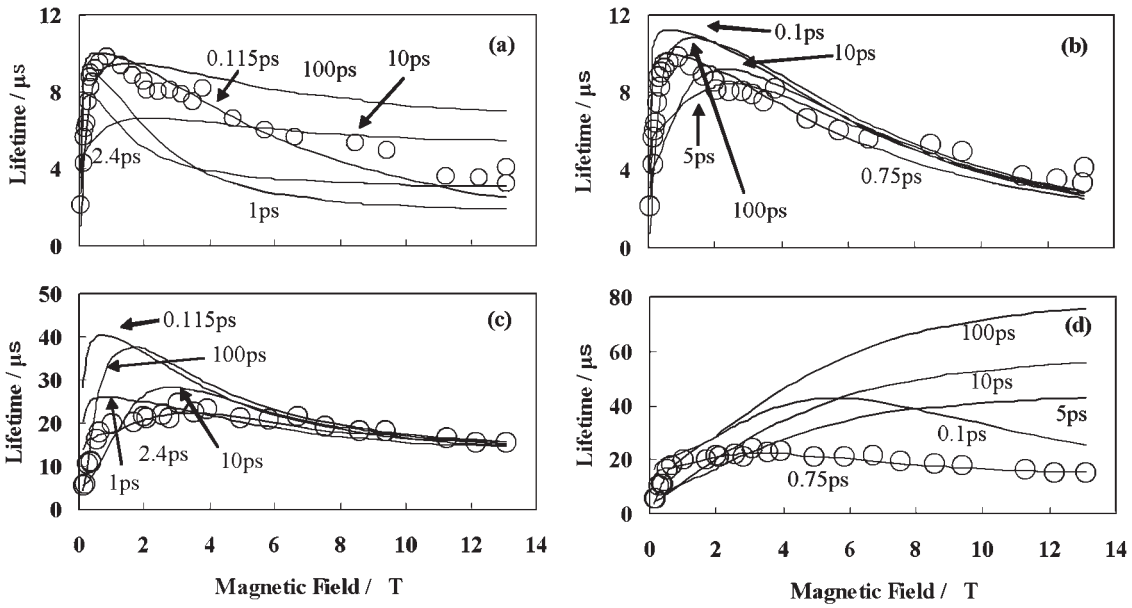

Fig. 5. Observed (○) and calculated (—) MFDs of the biradical lifetimes. The parameter of k_T is fixed at 8.50×10^4 s^{-1} in $Ph^{\bullet+}12V^{\bullet+}$ and 1.00×10^4 s^{-1} in $Cz^{\bullet+}12V^{\bullet+}$ during the model calculation. The parameters for the δg and δhf interactions in the calculated curves are $(g{:}g) = 181.8 \times 10^{-7}$, $(H_{loc}{:}H_{loc}) = 1.52$ mT^2, and $\tau_c = 0.115$ ps for $Ph^{\bullet+}$, $(g{:}g) = 20.01 \times 10^{-7}$, $(H_{loc}{:}H_{loc}) = 2.31$ mT^2, and $\tau_c = 0.75$ ps for $V^{\bullet+}$, and $(g{:}g) = 1.478 \times 10^{-7}$, $(H_{loc}{:}H_{loc}) = 2.26$ mT^2, and $\tau_c = 2.4$ ps for $Cz^{\bullet+}$, respectively. (a) Dependence of τ_c (0.115, 1, 2.4, 10, and 100 ps) for $Ph^{\bullet+}$ when $\tau_c = 0.75$ ps for $V^{\bullet+}$ in $Ph^{\bullet+}12V^{\bullet+}$. (b) Dependence of τ_c (0.1, 0.75, 5, 10, and 100 ps) for $V^{\bullet+}$ when $\tau_c = 0.115$ ps for $Ph^{\bullet+}$ in $Ph^{\bullet+}12V^{\bullet+}$. (c) Dependence of τ_c (0.115, 1, 2.4, 10, and 100 ps) for $Cz^{\bullet+}$ when $\tau_c = 0.75$ ps for $V^{\bullet+}$ in $Cz^{\bullet+}12V^{\bullet+}$. (d) Dependence of τ_c (0.1, 0.75, 5, 10, and 100 ps) for $V^{\bullet+}$ when $\tau_c = 2.4$ ps for $Cz^{\bullet+}$ in $Cz^{\bullet+}12V^{\bullet+}$.

fixing τ_c at 0.115 ps for $Ph^{\bullet+}$. The τ_c value, which well reproduces the observed MFD in the variation of τ_c, was applied to the fixed τ_c in the other calculation. Through such model calculations, the values for the unknown τ_c in $Ph^{\bullet+}12V^{\bullet+}$ were finally obtained to be 0.115 ps for $Ph^{\bullet+}$ and 0.75 ps for $V^{\bullet+}$ when $k_T = 8.50 \times 10^4$ s^{-1}. The curve simulated using these values in addition to $(g{:}g) = 181.8 \times 10^{-7}$ and $(H_{loc}{:}H_{loc}) = 1.52$ mT^2 for $Ph^{\bullet+}$ and $(g{:}g) = 20.01 \times 10^{-7}$ and $(H_{loc}{:}H_{loc}) = 2.31$ mT^2 for $V^{\bullet+}$ taken from Table 2 was well superimposed to the MFD observed in > 0.1 T of Fig. 3a. In conclusion, as well as the previous study, the importance of both such a very small τ_c and thereby the importance of local motions having the small τ_c were also confirmed in this study.

From a comparison between Figs. 5a and 5b, it was found that the fitting curves drawn above ca. 2 T in Fig. 5a, where the δg interaction dominantly works, shows high sensitivity to τ_c of $Ph^{\bullet+}$. On the contrary, the fitting curves in 0.1–2 T, where the δhf interaction contributes, widely deviates, depending on the τ_c of $V^{\bullet+}$, as depicted in Fig. 5b. Broadly speaking, therefore, it is not too much to say that the lifetimes of $Ph^{\bullet+}12V^{\bullet+}$ above ca. 2 T and in 0.1–2 T are governed by the δg interaction of $Ph^{\bullet+}$ and the δhf interaction of $V^{\bullet+}$, respectively. These assignments are proved by the experimentally observed MFDs that a great extent of the decrease above 1 T in $Ph^{\bullet+}12V^{\bullet+}$ was quite weakened and a gentle increase appeared anew in 1–3 T of $Cz^{\bullet+}12V^{\bullet+}$ when $Ph^{\bullet+}$ in $Ph^{\bullet+}12V^{\bullet+}$ was replaced by $Cz^{\bullet+}$ in $Cz^{\bullet+}12V^{\bullet+}$, as shown in Fig. 5c. In other words, the gentle increase that appeared in 1–3 T of $Cz^{\bullet+}12V^{\bullet+}$ is attributed to $Cz^{\bullet+}$. Furthermore, this interpretation is supported by the calculated values in Table 2. Since in the case of $Cz^{\bullet+}12V^{\bullet+}$ the largest $(g{:}g)$ value of $Ph^{\bullet+}$ was replaced by the smallest one of $Cz^{\bullet+}$, the δg interaction should be weakened, just leading to the small decrease in the lifetimes seen above 4 T. Judging from the result that the value of $(H_{loc}{:}H_{loc})$ for $Cz^{\bullet+}$ is relatively larger than $Ph^{\bullet+}$, as shown in Table 2, a gentle increase is necessarily expected to appear as well as the experimentally obtained MFD.

Similarly, the model calculations for the MFD of $Cz^{\bullet+}12V^{\bullet+}$ support the above-mentioned interpretation. In starting the model calculation, the values of $(g{:}g)$ and $(H_{loc}{:}H_{loc})$ for the respective radicals were taken from Table 2. As for the parameters for the dd interaction, the values for $Ph^{\bullet+}12V^{\bullet+}$ in Table 3 were used in return. As well as the case of $Ph^{\bullet+}12V^{\bullet+}$, k_T of $Cz^{\bullet+}12V^{\bullet+}$ in Figs. 5c and 5d was commonly fixed at 1.00×10^4 s^{-1} during the fitting calculation. In Fig. 5c, τ_c of $Cz^{\bullet+}$ was varied between 0.115 and 100 ps, while fixing τ_c for $V^{\bullet+}$ at a small value (0.75 ps) identical with that best fitted in $Ph^{\bullet+}12V^{\bullet+}$. Since $V^{\bullet+}$ is a common component between $Ph^{\bullet+}12V^{\bullet+}$ and $Cz^{\bullet+}12V^{\bullet+}$, it is no wonder that τ_c for $V^{\bullet+}$, estimated in $Ph^{\bullet+}12V^{\bullet+}$, is available for $Cz^{\bullet+}12V^{\bullet+}$. The value of 2.4 ps was obtained as the best in Fig. 5c through a calculation. It was already referred that the gentle increase seen in 1–3 T is attributable to the δhf interaction of $Cz^{\bullet+}$. This assignment was consistent with the result that the calculated curves varied largely in the same magnetic field region in Fig. 5c. In Fig. 5d, τ_c of $V^{\bullet+}$ was varied between 0.1 and 100 ps, while fixing τ_c at 2.4 ps for $Cz^{\bullet+}$, which is the best-fitted value obtained in Fig. 5c. The value of 0.75 ps was necessarily obtained as the best in Fig. 5d. The calculated curves in 2–14 T, where the δg interaction is predominant, were strongly dependent on τ_c of $V^{\bullet+}$, implying that the δg interaction inducing a slight decrease in the lifetime arose from $V^{\bullet+}$. Owing to the similarity in the $(H_{loc}{:}H_{loc})$ value between $Cz^{\bullet+}$ and $V^{\bullet+}$, a certain extent of change seen in the model calculations in Fig. 5d is understandable. Through these calculations, the values for the unknown τ_c in $Cz^{\bullet+}12V^{\bullet+}$ were finally obtained to be 2.4 ps for $Cz^{\bullet+}$ and 0.75 ps for $V^{\bullet+}$ when $k_T = 1.00 \times 10^4$ s^{-1}. The curve simulated using these values in addition to $(g{:}g) = 1.478 \times 10^{-7}$ and $(H_{loc}{:}H_{loc}) = 2.26$ mT^2 for $Cz^{\bullet+}$ and $(g{:}g) = 20.01 \times 10^{-7}$ and $(H_{loc}{:}H_{loc}) = 2.31$ mT^2 for $V^{\bullet+}$, taken from Table 2, was successfully superimposed to the observed MFD in Fig. 3b. In conclusion, the correlation time was found to be on order of $Cz^{\bullet+} > V^{\bullet+} > Ph^{\bullet+}$.

Finally, to verify the reliability of the calculated and estimated values for Eq. 8, it was checked whether the MFDs of $Ph^{\bullet+}12V^{\bullet+}$, $Ph^{\bullet+}10V^{\bullet+}$, and $Ph^{\bullet+}8V^{\bullet+}$ with different chain lengths (n) are reproducible with the values. As for the parameters for the dd interaction and k_T, they were varied depending on n (see Table 3). This is because the dd interaction and the SOC-induced recombination (Eq. 7), in which the latter rate constant is included into the magnetic-field-independent k_T, are dependent on the inter-radical distance. Figure 6 shows the n dependence of the MFDs of $Ph^{\bullet+}nV^{\bullet+}$, which was measured by direct laser excitation of the parent molecules ($PhnV^{2+}$). The reversal appeared in all of the MFDs. Here, by comparing Figs. 6a and 3a, it is conspicuous that the lifetimes of $Ph^{\bullet+}12V^{\bullet+}$ in them are different from each other. This discrepancy seems to be explained by a difference in the yield of the initial biradical formation. The biradical yield in the direct excitation is considered to be higher than in the triplet sensitization because of direct excitation, itself. Further, Yonemura and his co-workers pointed out the existence of magnetic-field-independent intermolecular back electron transfer between $Ph^{\bullet+}12V^{\bullet+}$ and $Ph12V^{2+}$, followed by the simultaneous formation of two kinds of mono-radical cations ($Ph^{\bullet+}12V^{2+}$ and $Ph12V^{\bullet+}$ in Eq. 6).[10,14] In the case of direct excitation, therefore, the bimolecular back electron-transfer reaction would effectively operate to decrease the biradical lifetime. Since this back electron-transfer process in Eq. 6 has no relation with the MFE mechanism, the decrease in the lifetime occurs in the same way regardless of the absence or presence of any magnetic fields, and thereby the difference between Figs. 6a and 3a is contained into the magnetic-field-independent k_T in Eq. 8. This means that in the triplet sensitization the calculated and estimated values for the individual parameters in Eq. 8, besides k_T, are available in their entirety for simulating the observed MFDs in Fig. 6. The solid lines in Fig. 6 depict the well-fitted curves obtained without any change in the parameters, except for k_T, indicating the reliability in the parameters estimated in this study. The used values for k_T were 1.60×10^5, 1.80×10^5, and 2.05×10^5 s^{-1} in $Ph^{\bullet+}12V^{\bullet+}$, $Ph^{\bullet+}10V^{\bullet+}$, and $Ph^{\bullet+}8V^{\bullet+}$, respectively. This trend obtained in k_T definitely reflects the experimental result that the lifetime in the presence of a magnetic field decreases as reducing n, because the lifetime is partly determined by k_T, as denoted in Eq. 8. This n dependence of k_T would be interpreted by the enhanced contribution of the SOC-induced recombination (Eq.

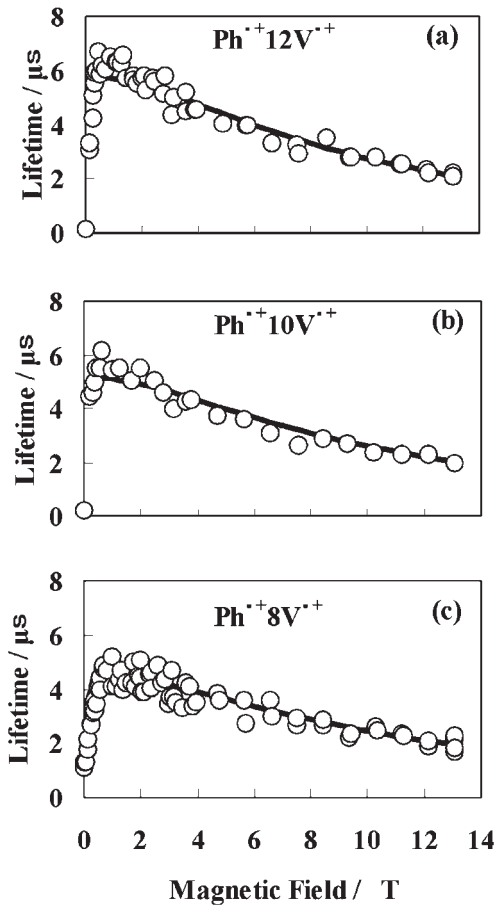

Fig. 6. Observed (○) and finally simulated (▬) MFDs of the biradical lifetimes in (a) $Ph^{\bullet+}12V^{\bullet+}$, (b) $Ph^{\bullet+}10V^{\bullet+}$, and (c) $Ph^{\bullet+}8V^{\bullet+}$. The parameters for the δg and δhf interactions in the simulated curves are $(g{:}g) = 181.8 \times 10^{-7}$, $(H_{loc}{:}H_{loc}) = 1.52$ mT^2, and $\tau_c = 0.115$ ps for $Ph^{\bullet+}$, $(g{:}g) = 20.01 \times 10^{-7}$, $(H_{loc}{:}H_{loc}) = 2.31$ mT^2, and $\tau_c = 0.75$ ps for $V^{\bullet+}$, respectively. The parameters for the dd interaction and k_T in the simulated curves are (a) $\overline{R^6} = 11.0 \times 10^6$ Å^6, $\tau_{c12} = 374$ ps, and $k_T = 1.60 \times 10^5$ s^{-1}, (b) $\overline{R^6} = 7.94 \times 10^6$ Å^6, $\tau_{c12} = 327$ ps, and $k_T = 1.80 \times 10^5$ s^{-1}, and (c) $\overline{R^6} = 3.36 \times 10^6$ Å^6, $\tau_{c12} = 211$ ps, and $k_T = 2.05 \times 10^5$ s^{-1}, respectively.

7) to k_T together with reducing n, since a part of k_T consists of the magnetic-field-independent process of Eq. 7, as already described in the explanation of Eq. 8. The SOC interaction becomes large when the component radicals approach each other. On the contrary, the lifetime at 0 T increases with reducing n. This n dependence can be understood by the enhanced exchange interaction as the inter-radical distance becomes short. When the inter-radical distance is long enough, the energy level of the triplet biradical is degenerate with that of the singlet one, meaning that the ISC rate in Eq. 4 is very fast (ca. 10^8 s^{-1}). Broadly speaking, therefore, the biradical lifetime at 0 T is determined by the process in Eq. 5, as already mentioned above. However, when the distance becomes short, the enhanced electron exchange interaction between the component radicals makes an energy gap (usually denoted as $2J$) between the triplet and singlet biradical levels, causing a deceleration in the ISC rate in Eq. 4. This means that the rate-determining stage, that is, the stage determining the lifetime, is replaced by Eq. 4 from Eq. 5. Although the enhanced SOC-induced recombination in Eq. 7 operates so as to make the biradical lifetime decrease, even at 0 T, the influence of the enhanced exchange interaction is interpreted to be large enough to cause an increase in the lifetime at 0 T in these reaction systems.

3. Conclusion

In this study, we applied quantum chemical calculations to delve into the high MFDs characteristic of the reversals. Through the model calculations, we have been able to mention the dominant interaction in the respective magnetic field regions: namely, $Ph^{\bullet+}12V^{\bullet+}$, the δhf interactions due to $V^{\bullet+}$ in 0.1–1 T and the δg interaction due to $Ph^{\bullet+}$; $Cz^{\bullet+}12V^{\bullet+}$, the δhf interaction due to $Cz^{\bullet+}$ in 1–3 T and the δg interaction due to $V^{\bullet+}$. Furthermore, we successfully demonstrated that two extremely small correlation times are absolutely necessary for interpreting the high MFDs characteristic of the reversals. The obtained correction time has been found to be in the order of $Cz^{\bullet+} > V^{\bullet+} > Ph^{\bullet+}$. However, such small correlation times can not be explained by the radical motion as a whole. Although we cannot exactly assign the origins of the small correlation times in the individual radicals at present, we have attempted to compare them from the viewpoint of the rigidity of the radical structure. The ring frame of $Cz^{\bullet+}$ is considered to be rigid enough to resist a local motion, such as a butterfly motion of the two phenyl rings. On the contrary, $Ph^{\bullet+}$ and $V^{\bullet+}$ have supple frameworks by a flexible structure inducing a butterfly motion of two phenyl rings in $Ph^{\bullet+}$ and a freely-rotated C–C bond linking two pyridyls in $V^{\bullet+}$, respectively. In fact, according to a quantum chemical calculation of the infrared frequencies, it has been verified that $Ph^{\bullet+}$ and $V^{\bullet+}$ have local motions like a butterfly motion and a rotation around the C–C bond, respectively. From these situations, it is not difficult to speculate the order in τ_c as being $Cz^{\bullet+} > V^{\bullet+}$ and $Cz^{\bullet+} > Ph^{\bullet+}$. Although at the moment we can't give a clear explanation for the smallness of τ_c, as described above, this successful comparison of the rigidity of the radical framework with τ_c might predict possibilities of local motions as the origin.

This work was partly supported by Grant-in-Aid for Scientific Research on Priority Area "Innovative utilization of strong magnetic fields" (Area 767, No. 15085208) from MEXT and partly by the Grant-in-Aid for Scientific Research (No. 15350016) from JPSP.

References

1 U. E. Steiner and H.-J. Wolff, "Photochemistry and Photophysics," ed by J. F. Rabek and G. W. Scott, CRC Press, Boca Raton, FL (1991), Vol. 4.

2 Y. Tanimoto and Y. Fujiwara, *J. Synth. Org. Chem. Jpn.*, **53**, 413 (1995).

3 "Dynamic Spin Chemistry," ed by S. Nagakura, H. Hayashi, and T. Azumi, Kodansya/Wiley, Tokyo (1998).

4 H. Hayashi, "Introduction to Dynamic Spin Chemistry: Magnetic Field Effects on Chemical and Biochemical Reactions," World Scientific, Singapore (2004).

5 Y. Tanimoto and Y. Fujiwara, "Handbook of Photochem-

istry and Photobiology," ed by H. S. Nalwa, American Scientific Publishers, USA (2003), Vol. 1, Chap. 10.

6 H. Hayashi and S. Nagakura, *Bull. Chem. Soc. Jpn.*, **57**, 322 (1984).

7 A. Abragam, "The Principles of Nuclear Magnetism," Clarendon Press, Oxford (1961), Chap. 8.

8 A. Carrington and A. D. McLachlan, "Introduction to Magnetic Resonance with Application to Chemistry and Chemical Physics," Harper and Row, New York (1967), Chap. 11.

9 Y. Fujiwara, T. Aoki, K. Yoda, H. Cao, M. Mukai, T. Haino, Y. Fukazawa, Y. Tanimoto, H. Yonemura, T. Matsuo, and M. Okazaki, *Chem. Phys. Lett.*, **259**, 361 (1996).

10 H. Yonemura, Ph.D. Thesis, Kyushu University, Japan (1995).

11 Y. Fujiwara, M. Mukai, T. Tamura, Y. Tanimoto, and M. Okazaki, *Chem. Phys. Lett.*, **213**, 89 (1993).

12 "Gaussian 03, Revision B.04," Gaussian, Inc., Pittsburgh PA (2003).

13 The data were taken from the following literature: a) "Landolt-Börnstein Numerical Data and Functional Relationships in Science and Technology New Series," ed by K.-H. Hellwege, Springer-Verlag, Heidelberg (1977), Group II, Vol. 9. b) M. R. Fuchs, E. Schleicher, A. Schnegg, C. W. M. Kay, J. T. Törring, R. Bittl, A. Bacher, G. Richter, K. Möbius, and S. Weber, *J. Phys. Chem. B*, **106**, 8885 (2002). c) G. Maier, H. P. Reisenaur, B. Rohde, and K. Dehnicke, *Chem. Ber.*, **116**, 732 (1983). d) F. L. Rupérez, J. C. Conesa, and J. Soria, *Spectrochim. Acta*, **40A**, 1021 (1984). e) Y. Itagaki and M. Shiotani, *J. Phys. Chem. A*, **103**, 5189 (1999).

14 H. Yonemura, H. Nakamura, and T. Matsuo, *Chem. Phys.*, **162**, 69 (1992).

15 The fluorescence lifetimes (τ_F*) of ^{1}Ph*12V^{2+} and ^{1}Cz*12V^{2+} were measured to be 1.51 and 3.8 ns, respectively.[10] The ISC rate constants (k_{ISC}*) in ^{1}Ph*12V^{2+} and ^{1}Cz*12V^{2+} were tentatively substituted with ones in the structural analogues of phenothiazine with an N–H bond and *N*-methylcarbazole, respectively. In phenothiazine, k_{ISC}* was estimated to be 4.8×10^8 s^{-1} with the relation of $k_{ISC}^* = \Phi_{T\text{-}ph}^*/\tau_{F\text{-}ph}^*$, where $\Phi_{T\text{-}ph}$* and $\tau_{F\text{-}ph}$* were the excited triplet quantum yield (0.44) and the fluorescence lifetime (0.91 ns), respectively, of phenothiazine in methanol [a) H. N. Ghosh, A. V. Sapre, D. K. Palit, and J. P. Mittal, *J. Phys. Chem. B*, **101**, 2315 (1997).]. On *N*-methylcarbazole in ethanol, $k_{ISC}^* = 3.74 \times 10^7$ s^{-1} was taken from the literature [b) S. M. Bonesi and R. Erra-Balsells, *J. Lumin.*, **93**, 51 (2001).]. Therefore, the excited triplet quantum yields (Φ_T*) of ^{3}Ph*12V^{2+} and ^{3}Cz*12V^{2+} were roughly evaluated to be 0.7 and 0.1, respectively, according to $\Phi_T^* = k_{ISC}^* \times \tau_F^*$. On the other hand, the decay rate constants of the molecules (^{3}Ph*12N$^+$(CH$_3$)$_3$2Br$^-$ and ^{3}Cz*12N$^+$(CH$_3$)$_3$2Br$^-$), which give rise to no electron transfer, were in the order of 10^3 and 10^4 s^{-1}, respectively. However, once the molecules acquire the electron acceptor of V^{2+}, namely, Ph12V^{2+} and Cz12V^{2+}, the rate constants were found to be beyond 10^8 s^{-1}. This is based on the biradical transient absorption signal appearing very fast within the time domain (<10 ns) of a nanosecond laser pulse used in the case of direct photo-excitation of Ph12V^{2+} and Cz12V^{2+}. This fact indicates that a quantum yield of the electron transfer reaction from the excited triplet states (^{3}Ph*12V^{2+} and ^{3}Cz*12V^{2+}) is infinitely close to unity. Thus, Φ_T* is considered to correspond to Φ_{BR}.

16 Y. Fujiwara, T. Aoki, Y. Tanimoto, H. Yonemura, S. Yamada, and T. Matsuo, Symposium on Photochemistry, Abstr., No. B105 (1997).

17 P. P. Levin and V. A. Kuzmin, *Chem. Phys.*, **162**, 79 (1992).